Passively Q-switched waveguide lasers based on two-dimensional transition metal diselenide

Chen Cheng,[1] Hongliang Liu,[1] Yang Tan,[1] Javier R. Vázquez de Aldana,[2] and Feng Chen[1,*]

[1]*School of Physics, State Key Laboratory of Crystal Materials, Shandong University, Jinan 250100, China*
[2]*Laser Microprocessing Group, Universidad de Salamanca, Salamanca 37008, Spain*
[*]*drfchen@sdu.edu.cn*

Abstract: We reported on the passively Q-switched waveguide lasers based on few-layer transition metal diselenide, including molybdenum diselenide ($MoSe_2$) and tungsten diselenide (WSe_2), as saturable absorbers. The $MoSe_2$ and WSe_2 membranes were covered on silica wafers by chemical vapor deposition (CVD). A low-loss depressed cladding waveguide was produced by femtosecond laser writing in a Nd:YAG crystal. Under optical pump at 808 nm, the passive Q-switching of the Nd:YAG waveguide lasing at 1064 nm was achieved, reaching maximum average output power of 115 mW ($MoSe_2$) and 45 mW (WSe_2), respectively, which are corresponding to single-pulse energy of 36 nJ and 19 nJ. The repetition rate of the Q-switched waveguide lasers was tunable from 0.995 to 3.334 MHz ($MoSe_2$) and 0.781 to 2.938 MHz (WSe_2), and the obtained minimum pulse duration was 80ns ($MoSe_2$) and 52 ns (WSe_2), respectively.

OCIS codes: (230.7370) Waveguides; (140.3390) Laser materials processing; (140.3540) Lasers, Q-switched.

References and links

1. R. Mas-Ballesté, C. Gómez-Navarro, J. Gómez-Herrero, and F. Zamora, "2D materials: to graphene and beyond," Nanoscale **3**(1), 20–30 (2011).
2. K. S. Novoselov, D. Jiang, F. Schedin, T. J. Booth, V. V. Khotkevich, S. V. Morozov, and A. K. Geim, "Two-dimensional atomic crystals," Proc. Natl. Acad. Sci. U.S.A. **102**(30), 10451–10453 (2005).
3. J. N. Coleman, M. Lotya, A. O'Neill, S. D. Bergin, P. J. King, U. Khan, K. Young, A. Gaucher, S. De, R. J. Smith, I. V. Shvets, S. K. Arora, G. Stanton, H. Y. Kim, K. Lee, G. T. Kim, G. S. Duesberg, T. Hallam, J. J. Boland, J. J. Wang, J. F. Donegan, J. C. Grunlan, G. Moriarty, A. Shmeliov, R. J. Nicholls, J. M. Perkins, E. M. Grieveson, K. Theuwissen, D. W. McComb, P. D. Nellist, and V. Nicolosi, "Two-dimensional nanosheets produced by liquid exfoliation of layered materials," Science **331**(6017), 568–571 (2011).
4. Q. H. Wang, K. Kalantar-Zadeh, A. Kis, J. N. Coleman, and M. S. Strano, "Electronics and optoelectronics of two-dimensional transition metal dichalcogenides," Nat. Nanotechnol. **7**(11), 699–712 (2012).
5. A. Splendiani, L. Sun, Y. Zhang, T. Li, J. Kim, C. Y. Chim, G. Galli, and F. Wang, "Emerging photoluminescence in monolayer MoS_2," Nano Lett. **10**(4), 1271–1275 (2010).
6. W. Zhao, R. M. Ribeiro, M. Toh, A. Carvalho, C. Kloc, A. H. Castro Neto, and G. Eda, "Origin of indirect optical transitions in few-layer MoS_2, WS_2, and WSe_2," Nano Lett. **13**(11), 5627–5634 (2013).
7. E. J. Murphy, *Intergrated Optical Circuits and Components* (Marcel Dekker, 1999).
8. A. Schaap, T. Rohrlack, and Y. Bellouard, "Optical classification of algae species with a glass lab-on-a-chip," Lab Chip **12**(8), 1527–1532 (2012).
9. E. Saglamyurek, N. Sinclair, J. Jin, J. A. Slater, D. Oblak, F. Bussières, M. George, R. Ricken, W. Sohler, and W. Tittel, "Broadband waveguide quantum memory for entangled photons," Nature **469**(7331), 512–515 (2011).
10. D. N. Christodoulides, F. Lederer, and Y. Silberberg, "Discretizing light behaviour in linear and nonlinear waveguide lattices," Nature **424**(6950), 817–823 (2003).
11. J. I. Mackenzie, "Dielectric solid-state planar waveguide lasers: A review," IEEE J. Sel. Top. Quantum Electron. **13**(3), 626–637 (2007).
12. S. Müller, T. Calmano, P. Metz, N. O. Hansen, C. Kränkel, and G. Huber, "Femtosecond-laser-written diode-pumped Pr:$LiYF_4$ waveguide laser," Opt. Lett. **37**(24), 5223–5225 (2012).
13. C. Grivas, C. Corbari, G. Brambilla, and P. G. Lagoudakis, "Tunable, continuous-wave Ti:sapphire channel waveguide lasers written by femtosecond and picosecond laser pulses," Opt. Lett. **37**(22), 4630–4632 (2012).
14. C. Grivas, "Optically pumped planar waveguide lasers, Part I: Fundamentals and fabrication techniques," Prog. Quantum Electron. **35**(6), 159–239 (2011).

#262093 Received 30 Mar 2016; revised 29 Apr 2016; accepted 29 Apr 2016; published 3 May 2016

15. C. Grivas, "Optically pumped planar waveguide lasers: Part II: gain media, laser systems, and applications," Prog. Quantum Electron. **45–46**, 3–160 (2016).
16. T. Calmano and S. Müller, "Crystalline waveguide lasers in the visible and near-infrared spectral range," IEEE J. Sel. Top. Quantum Electron. **21**(1), 1602213 (2015).
17. F. Chen and J. R. V. de Aldana, "Optical waveguides in crystalline dielectric materials produced by femtosecond-laser micromachining," Laser Photonics Rev. **8**(2), 251–275 (2014).
18. A. Okhrimchuk, V. Mezentsev, A. Shestakov, and I. Bennion, "Low loss depressed cladding waveguide inscribed in YAG:Nd single crystal by femtosecond laser pulses," Opt. Express **20**(4), 3832–3843 (2012).
19. G. Salamu, F. Jipa, M. Zamfirescu, and N. Pavel, "Watt-Level output power operation from diode-laser pumped circular buried depressed-cladding waveguides inscribed in Nd:YAG by direct femtosecond-laser Writing," IEEE Photonics J. **8**(1), 1500209 (2016).
20. T. Calmano, J. Siebenmorgen, A. G. Paschke, C. Fiebig, K. Paschke, G. Erbert, K. Petermann, and G. Huber, "Diode pumped high power operation of a femtosecond laser inscribed Yb:YAG waveguide laser," Opt. Mater. Express **1**(3), 428–433 (2011).
21. Y. Tan, A. Rodenas, F. Chen, R. R. Thomson, A. K. Kar, D. Jaque, and Q. Lu, "70% slope efficiency from an ultrafast laser-written Nd:$GdVO_4$ channel waveguide laser," Opt. Express **18**(24), 24994–24999 (2010).
22. Y. Tan, R. Y. He, J. R. Macdonald, A. K. Kar, and F. Chen, "Q-switched Nd:YAG channel waveguide laser through evanescent field interaction with surface coated graphene," Appl. Phys. Lett. **105**(10), 101111 (2014).
23. G. Della Valle, R. Osellame, G. Galzerano, N. Chiodo, G. Cerullo, P. Laporta, O. Svelto, U. Morgner, A. G. Rozhin, V. Scardaci, and A. C. Ferrari, "Passive mode locking by carbon nanotubes in a femtosecond laser written waveguide laser," Appl. Phys. Lett. **89**(23), 231115 (2006).
24. Y. Tan, Z. Guo, L. Ma, H. Zhang, S. Akhmadaliev, S. Zhou, and F. Chen, "Q-switched waveguide laser based on two-dimensional semiconducting materials: tungsten disulfide and black phosphorous," Opt. Express **24**(3), 2858–2866 (2016).
25. C. Cheng, H. L. Liu, Z. Shang, W. J. Nie, Y. Tan, B. R. Rabes, J. R. Vázquez de Aldana, D. Jaque, and F. Chen, "Femtosecond laser written waveguides with MoS_2 as satuable absorber for passively Q-switched lasing," Opt. Mater. Express **6**(2), 367 (2016).
26. R. I. Woodward, R. C. Howe, T. H. Runcorn, G. Hu, F. Torrisi, E. J. Kelleher, and T. Hasan, "Wideband saturable absorption in few-layer molybdenum diselenide ($MoSe_2$) for Q-switching Yb-, Er- and Tm-doped fiber lasers," Opt. Express **23**(15), 20051–20061 (2015).
27. B. Chen, X. Zhang, K. Wu, H. Wang, J. Wang, and J. Chen, "Q-switched fiber laser based on transition metal dichalcogenides MoS_2, $MoSe_2$, WS_2, and WSe_2.," Opt. Express **23**(20), 26723–26737 (2015).
28. J. J. Zayhowski and P. L. Kelley, "Optimization of Q-switched lasers," IEEE J. Quantum Electron. **27**(9), 2220–2225 (1991).
29. G. J. Spühler, R. Paschotta, R. Fluck, B. Braun, M. Moser, G. Zhang, E. Gini, and U. Keller, "Experimentally confirmed design guidelines for passively Q-switched microchip lasers using semiconductor saturable absorbers," J. Opt. Soc. Am. B **16**(3), 376–388 (1999).

1. Introduction

Recently, the two-dimensional (2D) nanomaterials, e.g. graphene and layered analogous to graphene, have received much attentions from the researchers in many areas due to the intriguing electronic and optical features [1–3]. Transition metal dichalcogenide (TMDC) possesses excellent properties for generations of photoluminescence, electroluminescence, ultrafast nonlinear absorption, second and third harmonics, which have been widely applied as key components in electronics and photonics [4,5]. In this family of 2D materials, Group VI transition metal (Mo, W and so on) diselenide as well as disulfide are the important members of the TMDCs owing to their direct band gap, with the structure of chalcogen atoms in two hexagonal planes separated by a plane of metal atoms [6].

Optical waveguides have been widely applied in many areas, such as modern telecommunication, quantum computing, information storage, and bio-sensing [7–9]. Due to the diffraction-free light propagation inside the waveguides, the beam manipulation could be achieved efficiently. A number of nonlinear optical applications (e.g., discrete solitons) might be realized in waveguides with diverse configurations that are absent in bulk systems [10]. Waveguides based on gain media have been utilized as the key components to obtain small-size, cost-effective miniature light sources in integrated photonic circuits [11]. Waveguide lasers, including continuous-wave (CW) and pulsed laser operation regimes, have been produced in a number of systems towards a broad range of photonic applications [12–17]. A significant first step of construction of waveguide laser systems is to fabricate waveguides in various gain media [17]. Recently, the femtosecond laser writing has become a powerful technique to manufacture waveguides with versatile geometries in more than 50 optical materials owing to its unique capability for 3D microstructuring and wide applicability for

#262093 Received 30 Mar 2016; revised 29 Apr 2016; accepted 29 Apr 2016; published 3 May 2016

diverse materials [16,17]. The laser written waveguide lasers in CW regimes have achieved excellent performances, such as high output powers, enhanced efficiencies, and reduced lasing thresholds [16–21]. More recently, research on pulsed waveguide lasers have also become more intriguing due to the rapid exploration of nanomaterials as broadband saturable absorbers (SAs) [22,23].Based on the nonlinear saturable absorption of nanomaterials, the passive Q-switching or mode-locking may be realized to achieve stable pulses through the waveguide cavities. A few nanomaterials, including graphene, single-wall carbon nanotubes (SWCN), disulfides (MoS_2 and WS_2), and black phosphorous, have been applied to achieve pulsed waveguide lasers in all-solid-state systems [22–25]. Particularly, in a laser-written Nd:YAG crystal waveguide with depressed cladding geometry, we have implemented Q-switched waveguide laser based on few-layer MoS_2 as SA at wavelength of 1064 nm [25]. Diselenides (both of $MoSe_2$ and WSe_2), contrast to disulfide TMDCs, have recently been shown to have excellent direct-gap semiconducting and non-linear optical properties, for instance a narrower gap semiconductor is required [4]. $MoSe_2$ and WSe_2 have been applied as SA materials in the Q-switched fiber lasers [26,27]. However, diselenides have not been used as SAs in waveguide laser systems up to now.

In this work, we reported on the all-solid-state Q-switched waveguide lasers in Nd:YAG based on few-layer $MoSe_2$ and WSe_2 thin-film mirrors. The lasing performance of the systems was investigated in details. A reasonable comparison was made between the $MoSe_2$ and WSe_2 waveguide laser systems, revealing clear discrepancy of the nonlinear absorption properties of two thin films. This work paves the way on the applications of 2D transition metal diselenides as excellent SAs in integrated waveguide laser platforms.

2. Experimental details

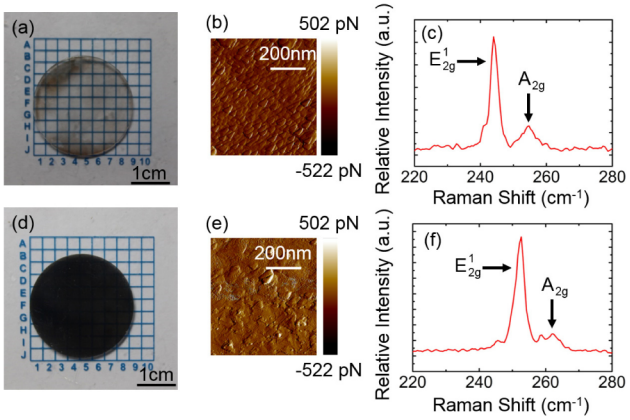

Fig. 1. Images of CVD $MoSe_2$ thin film (a) and WSe_2 (d) coated glass wafers. AFM images of $MoSe_2$ thin film (b) and WSe_2 (e). Raman spectra of the $MoSe_2$ thin film (c) and WSe_2 (f).

The Nd:YAG crystal (doped by 1 at.% Nd^{3+} ions) sample used in this work was cut into a wafer with dimension of 10 × 9 × 2 mm^3 and optically polished. The depressed cladding waveguide were written by an amplified Ti:Sapphire laser system, with pulse duration of 120 fs at a central wavelength of 800 nm with 1 kHz repetition rate. Details of Nd:YAG waveguide has been reported in [25].

The $MoSe_2$ and WSe_2 thin films were fabricated by the chemical-vapor-deposition (CVD) technology on fused silica wafers, which were commercial products (6Carbon Technology, Shenzhen, China). Few layers layout of $MoSe_2$ and WSe_2 membranes were utilized for ensuring the spatial integrity of the films and overspread the whole wafers. The photographs of wafers coated the $MoSe_2$ and WSe_2 thin films are exhibited in Figs. 1(a) and 1(d). The surface topography was characterized by an atomic force microscope (AFM) (shown in Figs. 1(b) and 1(e), respectively). The Raman spectra of $MoSe_2$ and WSe_2 membranes depict the

#262093 Received 30 Mar 2016; revised 29 Apr 2016; accepted 29 Apr 2016; published 3 May 2016

shifted peaks of the in-plane E1 2g vibration mode and out-plane A_{1g} vibration mode, which appear at 244.0 cm^{-1} and 254.7cm^{-1} in $MoSe_2$, and at 252.7 cm^{-1} and 260.3 cm^{-1} in WSe_2, respectively, as shown in Figs. 1(c) and 1(f).

The nonlinear absorption coefficients of the $MoSe_2$ and WSe_2 films were measured by the Z-scan technique with a 1064-nm laser with 22-ps pulse duration and 0.5-μJ energy and a lens (400mm-focal-distance). The experimental setup and process are same as [24]. The measured nonlinear transmissions of $MoSe_2$ and WSe_2 films are shown in Fig. 2(a). The relation between the transmission (T) and the excitation energy (I) has been fitted by the following equation

$$T(I) = 1 - \Delta T \times e^{-\frac{I}{I_{sat}}} - T_N \qquad (1)$$

where T_N is the nonsaturable absorbance, ΔT is modulation depth, and I_{sat} is saturable intensity. The values of ΔT and I_{sat} are 11.4% (5.4%) and 0.006 GW/cm^2 (0.007 GW/cm^2) for $MoSe_2$ (WSe_2). The damage thresholds of $MoSe_2$ and WSe_2 are higher than 0.05 GW/cm^2.

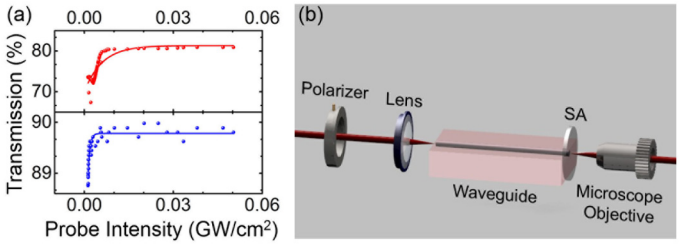

Fig. 2. (a) The nonlinear transmission as a function of the probe light intensity of $MoSe_2$ (red) and WSe_2 (blue), and (b) schematic of the experimental setup for the Q-switched waveguide laser generation.

We utilized a linearly polarized light beam at 808 nm generated from a tunable CW Ti:Sapphire laser (Coherent MBR PE) as the pump source. A thin film was coated on end face towards the pump source with parameters of high reflectivity at ~1064 nm and high transmission at ~808 nm. A 30mm-focal-length lens and a 20 × microscope objective lens (N.A. = 0.4) were used to launch the pump beam and collect the output lasers, respectively. The $MoSe_2$ and WSe_2 films were set as an output coupler mirror, the method was same as [24,25]. The detective devices were located after objective lens at the end of experimental system, including an infrared CCD for imaging, an oscilloscope, and a spectrometer. Figure 2(b) depicts the experimental setup of waveguide laser generation.

3. Results and discussion

Figures 3(a)-3(c) show the experimental results of the waveguide lasing based on both $MoSe_2$ and WSe_2 SAs. The average output power is illustrated as function of incident power in Fig. 3(a). From the linear fit of the experiment data, the slope efficiencies are determined to 26.4% and 26.5% and maximum output average power values are 115.1 mW and 105.7mW at TE- and TM-polarized (rectangle and circular symbols, respectively) pump via using $MoSe_2$-based SA (red lines and points). Whilst with WSe_2 SA (blue lines and points), the slope efficiencies are 7.4% and 7.0% and maximum output average power values are 45.7 mW and 42.7 mW, respectively. The minimum lasing thresholds are 189.7 mW (WSe_2) and 275.1 mW ($MoSe_2$).

The repetition rates of the Q-switched waveguide laser system are exhibited in Fig. 3(b), as function of incident pump power, which are tunable ranging from 0.995 to 3.334 MHz ($MoSe_2$) and 0.781 to 2.938 MHz (WSe_2) as the incident power into waveguide increases from 190 mW to 720 mW. Figure 3(c) shows the laser emission spectrum from Nd:YAG crystalline waveguide with $MoSe_2$ as SA. The central wavelength for the Q-switched lasers is 1064 nm for both TE- and TM-polarization, which clearly denotes the laser oscillation line that corresponds to the main fluorescence of $^4F_{3/2} \rightarrow {}^4I_{11/2}$ transition of Nd^{3+} ions. The full

#262093 Received 30 Mar 2016; revised 29 Apr 2016; accepted 29 Apr 2016; published 3 May 2016

width at half maximum (FWHM) value of the emission line is ~0.5 nm. In case of WSe_2 SA, the same laser spectrum at main emission line of 1064 nm has been obtained for TE and TM polarized pump. The inset two images present modal profiles of the two systems of waveguide lasers.

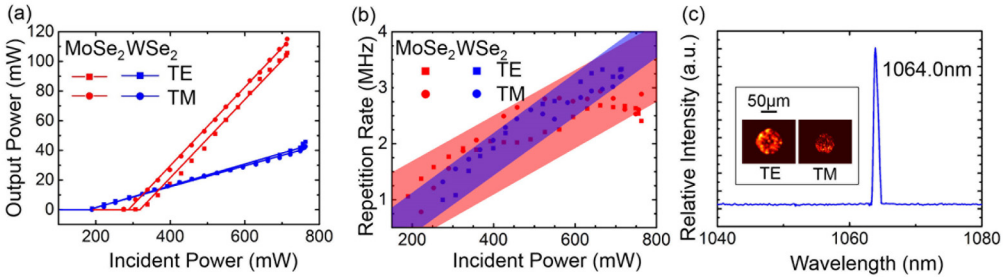

Fig. 3. The average output power (a) and repetition rate (b) of the Q-switched waveguide lasers as $MoSe_2$ (red lines and points) and WSe_2 (blue lines and points) based SAs at TE- (rectangle symbols) and TM-polarization (circular symbols); the Q-switched waveguide laser emission spectrum (c), based on $MoSe_2$ SA. The inset pictures show the output modal profiles from waveguide at TE- and TM-polarized light pump.

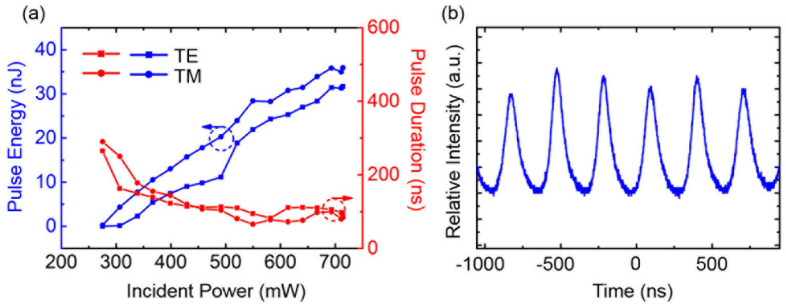

Fig. 4. Based on $MoSe_2$ SA, the Q-switched waveguide laser pulse energy and duration (a), and the pulse trains (b).

Using $MoSe_2$ as SA, the Q-switched laser details are depicted in Figs. 4(a) and 4(b) at room temperature, including pulse energy, pulse duration, and pulse train. The maximum single pulse energy is 35.9 nJ at TM-polarized light pump (the value is 31.7 nJ at TE-polarization). The pulse durations are in a range from 80 ns to 290 ns at TM-polarized light pump (the value from 86 ns to 265 ns corresponding to TE-polarization), as shown in Fig. 4(a). The typical oscilloscope traces of the Q-switched pulse train, at the incident power of ~667 mW TE-polarized pumping, have been shown in Fig. 4(b).

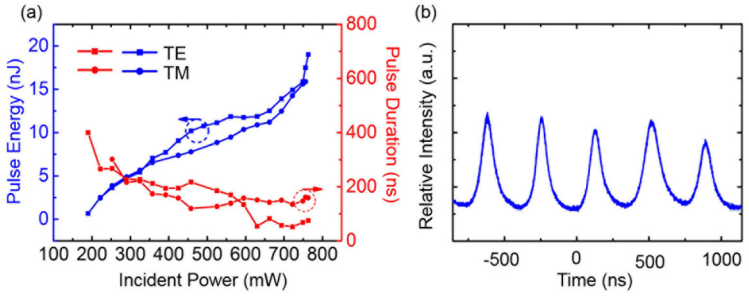

Fig. 5. Based on WSe_2 SA, the Q-switched waveguide laser pulse energy and duration (a), and the pulse trains (b).

#262093 Received 30 Mar 2016; revised 29 Apr 2016; accepted 29 Apr 2016; published 3 May 2016

Figures 5(a) and 5(b) show the details of Q-switched lasers based on WSe_2 SA under the same experimental conditions of $MoSe_2$. Figure 5(a) reveals that the maximum single pulse energy is 19.0 nJ at TE-polarized light pump (15.9 nJ at TM-polarization). The pulse durations are ranging from 52 ns to 400 ns at TE-polarized light pumping (from 135 ns to 301 ns at TM-polarization). The typical oscilloscope traces of the Q-switched pulse train, at the incident power of ~457.8 mW TE-polarized pumping, have been shown in Fig. 5(b).

Based on the results above, the modulation depths of Q-switched laser based on the two materials as SAs can be calculated, which was expressed as [28,29]

$$E_p \approx \frac{h\nu_L}{\sigma_L} Aq\eta_{out} \tag{2}$$

where E_P is the pulse energy; $h\nu_L$ is the photon energy at the laser wavelength; σ_L is the emission cross section of the laser material; A is the cross section of pumping volume; q is the modulation depth of SA; η_{out} is the coupling efficiency. As all parameters of the material and the waveguide, the values of modulation depth (q) can be calculated, which are 2.3% and 2.6% at TE- and TM-polarization pumping modulated by $MoSe_2$, corresponding 4.9% and 4.0% modulated by WSe_2.

Table 1. Comparison of Q-switched Waveguide Lasers Based on Different Nanomaterials as SAs

	Nanomaterials				
Parameters	MoS_2[a]	WS_2[b]	BP[b]	$MoSe_2$	WSe_2
Lasing Threshold (mW)	260.0	90.0	100.0	189.7	275.1
Pulse Duration (ns)	203	24	55	86	52
Repetition Rate (MHz)	1.100	6.100	5.600	3.334	2.938
Single Pulse Energy (nJ)	89	-	-	35.9	19.0
Modulation Depth	-	1.8%	0.8%	2.6%	4.9%

[a]From [25] and [b]from [24].

A comparison of Q-switched waveguide lasers based on different SA materials has been demonstrated in Table 1. It is worth mentioning that the waveguide laser based MoS_2 as SA (in Table 1) is on a same design of waveguide and cavity as this work. Compared with MoS_2, the waveguide lasers based on $MoSe_2$ and WSe_2 of SAs have been obtained shorter pulse durations and ~3 times repetition rate at a same Q-switched waveguide platform. For different waveguide laser designs, as [25], the deeper modulation depths were achieved in SAs of $MoSe_2$ and WSe_2. In addition, the WSe_2-based laser is with higher threshold but superior lasing performance than $MoSe_2$-based system.

Compared with Q-switched fiber lasers, all waveguide lasers have shown obvious advantage based on TMDCs of SAs. More optimized laser parameters, including megahertz-level repetition rates, nanosecond-level pulse durations, and hundred-milliwatt-level output powers, can be achieved under roughly equivalent pump light powers on the waveguide laser platform, compared with fiber lasers [26,27].

4. Summary

In conclusion, by using $MoSe_2$ and WSe_2 as SAs, the passively Q-switched waveguide lasers at 1064 nm have been implemented in laser written Nd:YAG depressed cladding waveguide. The waveguide lasers were with tunable repetition rates, low lasing thresholds, and nanosecond-level pulse durations. The Q-switched lasers based on transition metal diselenide as SAs imply more compact sizes of the waveguide laser systems that may be used as miniature light sources in photonic chips for diverse applications.

Acknowledgments

The work is supported by the National Natural Science Foundation of China (NSFC) (No. 11274203) and Junta de Castilla y León under Project SA086A12-2. Support from the Centro de Láseres Pulsados (CLPU) is also acknowledged.

#262093 Received 30 Mar 2016; revised 29 Apr 2016; accepted 29 Apr 2016; published 3 May 2016